A Study of the Mechanical and Electrical Properties of a Polymer/Carbon Black Binder System Used in Battery Electrodes

Zonghai Chen[1], L. Christensen,[2] J. R. Dahn[1,3]

[1]*Department of Chemistry, Dalhousie University, Halifax, Nova Scotia B3H 3J5, Canada*
[2]*3M Company, 3M Center, St. Paul, Minnesota, 55144-1000*
[3]*Department of Physics, Dalhousie University, Halifax, Nova Scotia B3H 3J5, Canada*

Received 7 October 2002; accepted 30 January 2003

ABSTRACT: The effects of carbon black content and crosslinking on the mechanical and electrical properties of a fluorinated elastomer, FC2178 (Dyneon Corp., Oakdale, MN), poly(vinylidene fluoride-*co*-hexafluoropropylene), were investigated and compared to those of poly(vinylidene fluoride) (PVDF). Attention was given to changes in mechanical and electrical properties of the polymers when under cyclic deformation. To describe the mechanical properties of the carbon-filled polymers in a way that is independent of the chemical details, two mechanical models were used to fit cyclic stress–strain experiments. The linear model was used to determine the effect of crosslinking on the mechanical properties of crosslinked FC2178 films. However, when carbon black was added to the polymer films, the linear model no longer fit the data well. In particular, the cyclic stress–strain curves for carbon-filled polymers showed non-linear regions and displayed the characteristic of 'memory.' A non-linear element was added in parallel with the existing elements of the linear model to successfully describe the effects of the added carbon black. © 2003 Wiley Periodicals, Inc. J Appl Polym Sci 90: 1891–1899, 2003

Key words: crosslinking; mechanical properties; modeling

INTRODUCTION

Carbon-filled polymer composites have been attracting a great deal of scientific research and industrial interest for many years because of their excellent mechanical and electrical properties.[1–7] The mechanical and electrical properties of carbon-filled composites are strongly affected by the morphology of the carbon fillers,[8] the dispersion quality,[9] the strain history[10,11] and the chemical treatment (i.e. crosslinking) of the composites. Generally, the chemical treatment techniques adopted include grafting or crosslinking of the polymer[12,13] and surface modification of carbon fillers.[14–16] It is of great utility to describe the mechanical properties of the polymer and its composites with a model instead of the chemical and experimental details of the composites.

Carbon black-filled polymer composites have been used in lithium-ion batteries as an electrode binder to maintain physical integrity and to help maintain an electrical pathway between active material particles and current collector.[5–7] The mechanical and electrical properties of the carbon-filled polymeric binder may therefore affect the performance of lithium-ion and other batteries.

The mechanical properties of carbon-filled binders for lithium battery electrodes have been given little or no attention in the literature. Commercially used active materials, such as $LiCoO_2$ and graphite, have small volumetric changes (<10%) during charging and discharging cycles. The mechanical properties of commonly used binders, such as poly(vinylidene fluoride) (PVDF), have not been challenged in these applications.

Tin-based compounds[17–21] have been proposed as high capacity anode materials for lithium-ion batteries. Tin-based compounds can provide a gravimetric capacity of more than 600 mAh/g[19], while the commercialized graphite electrode provides only 372 mAh/g. Hence, tin-based compounds have been investigated extensively. However, tin-based anode materials experience capacity loss with increasing cycle number, which is believed to be caused by their large volumetric changes (up to 255%) during charge/discharge cycling.[17,20,21] In electrode applications with large volumetric changes, a good binder system should be highly extensible and durable to tolerate the shape changes of the electrode during charge/discharge cycles. In this case, the mechanical properties of the binder become important.

It is our long-term goal to determine the relationship between the mechanical properties of the binder

Correspondence to: J. Dahn (jeff.dahn@dal.ca).

Journal of Applied Polymer Science, Vol. 90, 1891–1899 (2003)

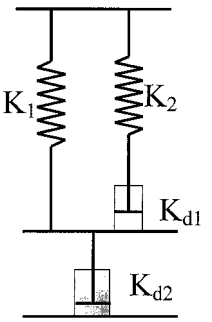

Figure 1 Schematic of the linear model used to describe the mechanical properties of polymer films. K_1 and K_2 are the spring constants in the model and K_{d1} and K_{d2} are constants used to characterize the viscosity of the dashpots in the model.

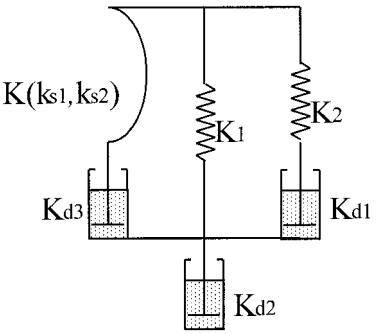

Figure 2 Schematic of the non-linear model used to describe the mechanical properties of polymer/carbon black films. K_1 and K_2 are the spring constants in the model, and K_{d1}, K_{d2} and K_{d3} are constants used to characterize the viscosity of the dashpots in the model. $K(K_{s1},K_{s2})$ describes the stiffness of the non-linear element. The parameters K_{s1} and K_{s2} are described in eq. (1).

system and the electrochemical performance of the resulting electrode. As a first step, it is important to describe the mechanical properties of the binder system with a suitable mechanical model. As a baseline, we first report the mechanical and electrical properties of carbon-filled PVDF, the binder currently used in many lithium-ion cell electrodes. Then, the mechanical properties of a fluorinated copolymer binder, poly(vinylidene fluoride-*co*-hexafluoropropylene) (FC2178, Dyneon, Oakdale, MN) are reported as a function of carbon black loading and crosslinking. Two mechanical models are used to describe the mechanical properties of the crosslinked polymer and polymer/carbon black blends, respectively.

Mechanical Models

Linear Model

Figure 1 shows a schematic of a four-element linear model.[22] In the linear model, K_1 and K_2 are the Young's moduli of springs used to represent the strength of the polymer, while K_{d1} and K_{d2} are constants for the dashpots used to model the viscosity of the polymer. This linear model[22] was used to study the mechanical properties of the FC2178 polymer and the effect of crosslinking in the absence of carbon black.

Non-linear Model

Normally, carbon black is used in polymers and binders as a conductive filler. In our study, when carbon black was added to the polymer, the mechanical properties changed dramatically and the linear model could no longer fit the cyclic stress–strain experiments properly. A non-linear element was needed to describe the effect of carbon black. Figure 2 shows a schematic of the non-linear model. Compared to the linear model, the non-linear model has a non-linear element placed in series with a third dashpot. The stress of the non-linear element, σ_n, is described by two parameters, k_{s1} and k_{s2} as in eq. (1):

$$\sigma_n = \begin{cases} k_{s1}\epsilon & \epsilon \geq \epsilon_{\max} \\ k_{s1}\epsilon_{\max} - k_{s2}(\epsilon_{\max} - \epsilon) & \epsilon_e < \epsilon \leq \epsilon_{\max} \\ 0 & \epsilon \leq \epsilon_e \end{cases} \quad (1)$$

where ϵ is the strain, $\epsilon_{\max}$ is the largest strain applied in the deformation history and ϵ_e is the strain at which a new equilibrium length of the non-linear element is established.

Figure 3 shows a diagram of the stress–strain behavior of the non-linear element as described by eq. (1) with an ϵ_e value of 0.4. Physically, the non-linear element is meant to represent a carbon black strand

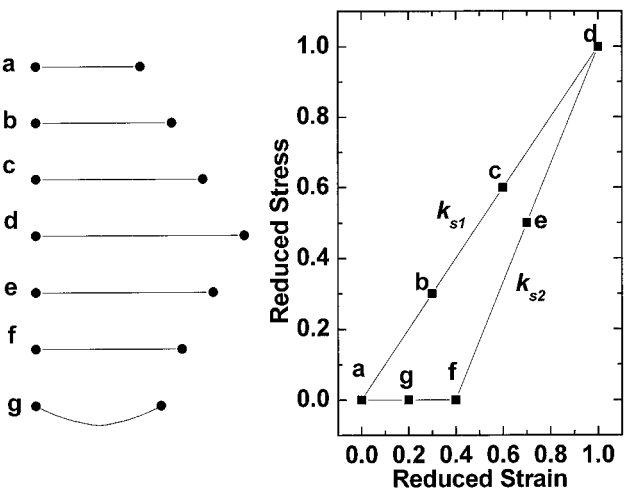

Figure 3 Stress–strain curve of the non-linear element proposed in this work: (a) initial state of the non-linear element; (a)–(d) stretched non-linear element, which is taut; (d)–(f) releasing but taut non-linear element; (f) non-linear element with its new equilibrium length; and (g) slack element if further released.

connected to viscoelastic polymer at each end. As the element is stretched, the carbon black strand rotates to be parallel to the stretching direction, thus establishing a new, longer equilibrium length. When the stress is removed, the polymer contracts, but we assume the carbon black strand does not rotate fully back to the original position and the element goes slack at point *f* in Figure 3. Although this non-linear element is empirically derived, we will show that it describes the main behavior of the carbon black-filled polymer studied here.

EXPERIMENTAL

Preparation of Binder and Binder/Solids Film

Two polymers, PVDF (Solef 1008/1001, Concord, Ontario, Canada) and FC2178 (Dyneon Corp.), were used as binders in this study. FC2178 is a copolymer of $CF_2{=}CH_2$ (VDF) and $CF_2{=}CF{-}CF_3$ (HFP). After the polymer was completely dissolved [in acetone (Aldrich, Oakville, Ontario, Canada) for FC2178 or N-methyl pyrrollidinone (Aldrich) for PVDF] and mixed with Super-S carbon black (SS) (MMM Carbon, Belgium), a measured amount of crosslinking agent, triethylenetetramine (TETA, Aldrich), was added. The final mixture was coated on a piece of copper foil using a notch bar spreader with a gap of 0.016 in. After spreading, the films containing FC2178 were dried overnight in air while films containing PVDF were dried at 110°C overnight. Finally, the copper foil was dissolved with 2*M* HNO_3. The typical thickness of the resulting free-standing films was about 0.06 mm. The amounts of SS and TETA in the films are reported in units of parts per hundred by polymer mass (pph).

Measurement of Mechanical Properties

The stress–strain and resistance–strain curves of the polymer films were collected simultaneously using a homemade stress–strain tester, which is schematically shown in Figure 4. Using a motion controller, the computer controls the motion of the actuator to cyclically stretch and release the binder film. The load cell transfers the force it experiences into a potential signal. There are two leads connected to both ends of binder film via grips. These leads are used to measure the resistance of the film. The multimeter collects the signals from both the load cell and the resistance leads and converts them into digital signals for the computer.

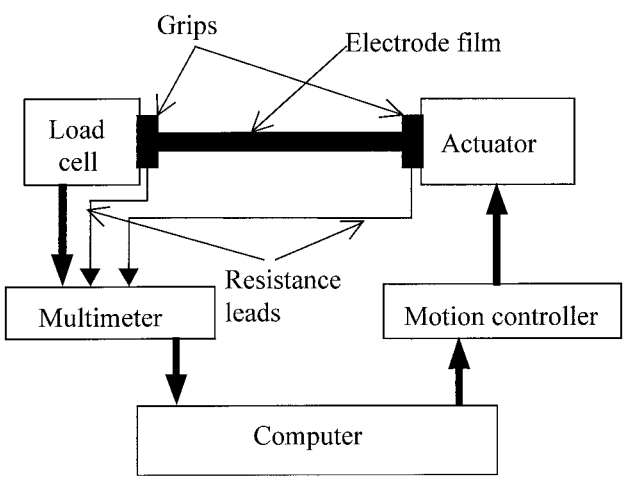

Figure 4 A schematic of the homemade stress–strain tester.

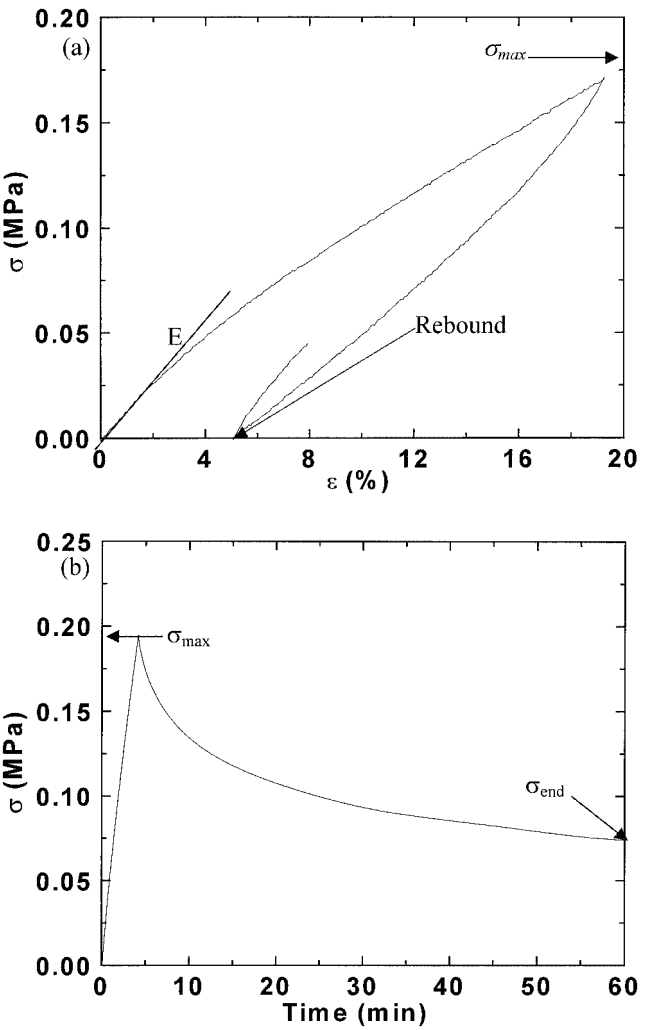

Figure 5 Definition of parameters discussed in the text: (a) stress–strain curve; (b) stress relaxation curve for an initial strain of 20%.

Figure 5 defines some parameters used in this study. Figure 5(a) shows a typical experimental stress–strain curve during cyclic deformation. Three parameters are used to describe the stress–strain curve. The Young's modulus, *E*, is the slope of the stress–strain curve at a small strain. The maximum stress, σ_{max}, is the stress measured at maximum strain during a cyclic deformation or relaxation test. The rebound is the value of the strain where the stress–strain curve

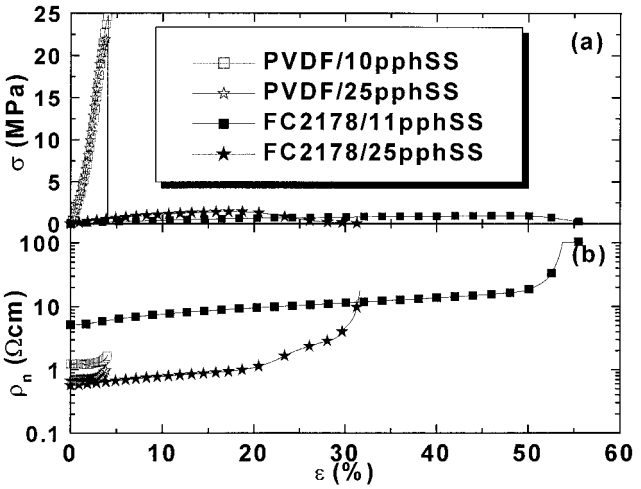

Figure 6 The elongation at break behavior of PVDF/SS and FC2178/SS films: (a) stress vs. strain, and (b) nominal resistivity vs. strain.

reaches zero stress at the end of the first deformation cycle. Figure 5(b) shows the relaxation of the applied stress at a fixed strain as a function of time. Two parameters, σ_{max} and σ_{end} are used to define the amount of relaxation that occurs in a specific time. We define the relaxation as

$$\text{Relaxation} = \frac{\sigma_{max} - \sigma_{end}}{\sigma_{max}} \times 100\% \quad (2)$$

The amount of relaxation depends on the time of the experiment. Normally, we measure the amount of relaxation that occurs in 60 min.

The nominal resistivity, ρ_n, is another important property of the binder/solid film. We define nominal resistivity as

$$\rho_n = \frac{RA_0}{L_0} \quad (3)$$

where R is the measured resistance of the binder/solid film, and A_0 and L_0 are the original cross-sectional area and the length of the film, respectively.

All stress–strain curves reported here were measured using a strain rate of 1% per minute. These slow rates were chosen to mimic the conditions within a lithium-ion battery, where electrode expansion and contraction cycles are on the order of one hour.

RESULTS AND DISCUSSION

Poor Mechanical Properties of PVDF compared to FC2178

Figure 6 compares the mechanical properties of PVDF and FC2178. Figure 6(a) shows the stress versus strain curves for PVDF/carbon black and FC2178/carbon black films stretched to the breaking point. The PVDF films with both 10 pph and 25 pph of SS can only be stretched to about 4% before breaking. The extensibility is quite poor. Compared to the PVDF/SS films, the FC2178/SS films have much better elongation before break. The FC2178 film with 11 pph SS can be extended to about 50% strain without breaking. Even when 25 pph SS is added, the film can be stretched to about 20% before breaking. Figure 6(b) shows the nominal resistivity versus strain of the PVDF/SS films and the FC2178/SS films. When the SS content increases from 10 pph to 25 pph, the nominal resistivity of the PVDF/SS and FC2178/SS films decreases by a factor of about 2.

Effect of Carbon Black on the Properties of FC2178

Figure 7(a) shows the effect of SS content on the mechanical properties of FC2178/SS films. As the SS content increases, the Young's modulus of the FC2178/SS film increases and the maximum elongation before break decreases significantly. When 5.2 pph SS was used, the film could be elongated by 60% before breaking. However, the film with 25 pph SS could only be stretched by 20%. Figure 7(b) shows the effect of SS content on the nominal resistivity of the FC2178/SS films. As the SS content increases, the resistivity decreases. The nominal resistivity increases with the strain applied.

The active material is an essential component of electrodes for lithium-ion batteries. The addition of active materials (normally $>$ 400 pph) will dramatically degrade the mechanical properties of the binder film, as the addition of SS does. Hence, the mechanical properties of the FC2178/SS system may not be sufficient for applications with large volumetric changes.

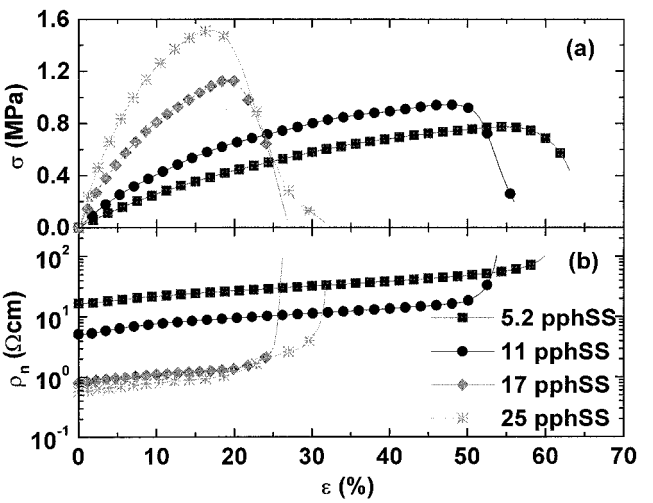

Figure 7 The effect of SS content on the breaking behavior of FC2178/SS films: (a) stress vs. strain, and (b) nominal resistivity vs. strain.

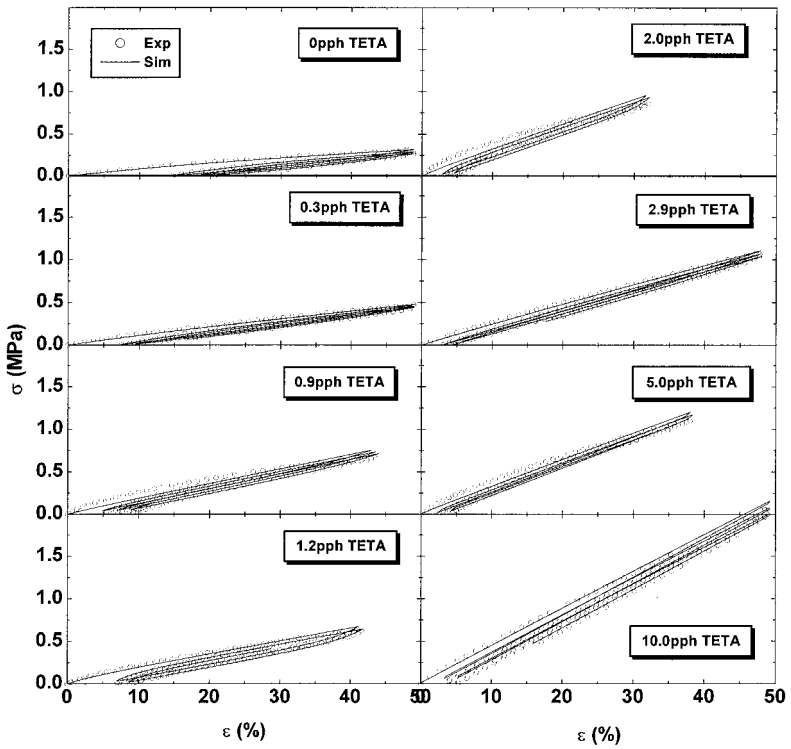

Figure 8 Stress vs. strain of FC2178 films with added TETA, showing the effect of TETA. Circles show experimental data and solid lines show calculated best-fit using the linear model.

Fortunately, the mechanical properties of FC2178/carbon black films can be significantly improved by crosslinking.

Crosslinking of FC2178 with TETA

A series of FC2178 films were prepared with different TETA contents, which ranged from 0 to 10 pph. The stress–strain curves collected are shown in Figure 8. All curves were fitted to the linear model, and the fitted results are shown in Figure 8 for comparison. As the TETA content increases, the Young's modulus of the binder film increases and the rebound point decreases. When 10 pph TETA were used, the stress–strain curve was almost linear, and rebounded to a very small strain (about 3%). This sample almost behaves as a Hooke's-law spring.

The parameters used to fit the linear model to the data in Figure 8 are listed in Table I. Figure 9 shows the fitted parameters plotted as a function of TETA content. The parameters, K_2 and K_{d1} do not show a clear trend with the TETA content. However, K_1 and K_{d2} show a strong dependence on the TETA content. They increase linearly when the TETA content is less than 4 pph, and continue to increase more slowly when more than 4 pph TETA are used. These parameters increase because the films are getting stiffer (K_1) and more viscous (K_{d1}).

Figure 10 shows the effect of TETA content in FC2178 films on the maximum stress at a given strain, the rebound point from the same strain and the relaxation in stress of films held at fixed strain. The maximum stress at fixed strain increases with TETA content when less than 3 pph TETA are used [Fig. 10(a)]. The rebound point and the amount of relaxation decrease with TETA content. When the TETA content is larger than 3 pph, the rebound point is less than 10% strain [Fig. 10(b)] and the amount of stress relaxation is constant, at near 10% [Fig. 10(c)]. Crosslinking with TETA not only increases the strength of the polymer films but also suppresses the viscous flow of the poly-

TABLE I
Best-Fit Parameters of the Linear Model to the Crosslinked FC2178 Films

TETA Content (pph)	K_1 (MPa)	K_2 (MPa)	K_{d1} (10^2 MPa s)	K_{d2} (10^5 MPa s)
0.0	0.70	0.81	4.1	0.14
0.3	0.89	0.30	3.6	0.77
0.9	1.8	0.85	1.5	1.1
1.2	1.6	1.3	3.8	0.81
2.0	3.0	1.9	2.7	1.9
2.9	3.7	10	3.2	2.0
5.0	3.2	3.1	1.2	2.5
10.0	4.4	16	0.68	3.6

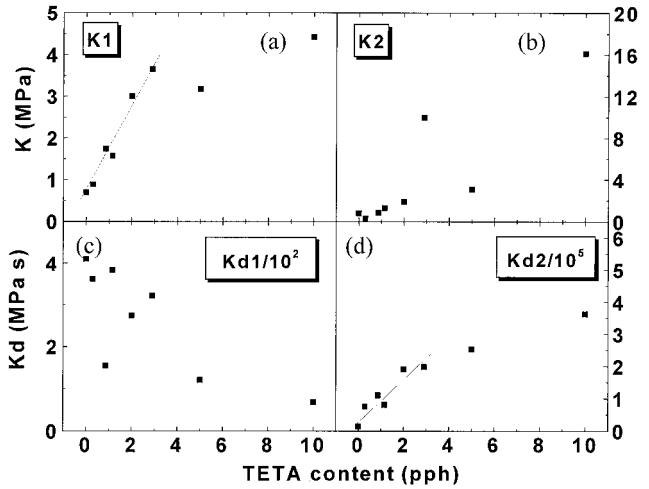

Figure 9 The effect of crosslinking on the parameters of the linear model for FC2178 films: (a) K_1 vs. TETA content, (b) K_2 vs. TETA content, (c) K_{d1} vs. TETA content, and (d) K_{d2} vs. TETA content.

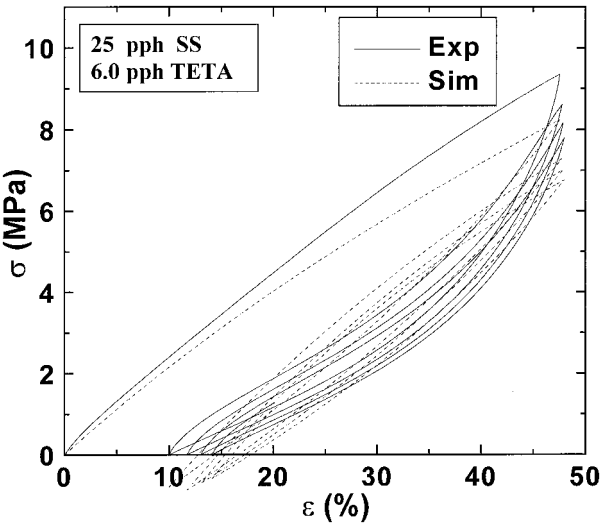

Figure 11 An attempt to describe the stress–strain curve of FC2178 with 25 pph SS and 6.0 pph TETA using the linear model.

mer chains. However, the improvement of the mechanical properties slows down when the TETA content is above 3 pph.

Introducing the Non-linear Element in the Mechanical Model

Solids like carbon black and active materials are essential components of the electrode. We would like to be use the mechanical model to describe films similar to electrodes. However, the linear model does not describe the data well when SS is added to the polymer. Figure 11 shows the poor agreement between the theoretical and experimental results, using the linear model, for a FC2178/TETA film containing 25 pph SS. The best-fit parameters for the linear model are listed in the first row of Table II. After the first stretch, the experimental curve shows sharply rising regions when the strain is larger than 40%. This corresponds to an increase in the modulus of the binder film. However, the theoretical results do not show this behavior. Under the extreme condition that the dashpot viscosities are infinite, the linear model reduces to a spring with a constant modulus. There is no way to explain the upward curvature in the experiment with the linear model. Thus, the linear model cannot simulate the regions of increasing modulus, and a non-linear element is needed to describe this behavior.

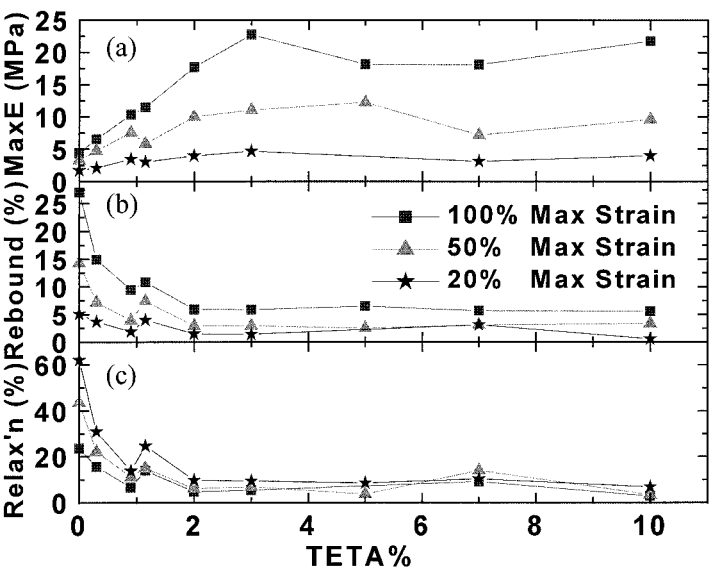

Figure 10 The effect of TETA on the mechanical properties of FC2178 films: (a) maximum stress vs. TETA content, (b) rebound point vs. TETA content and (c) percent stress relaxation vs. TETA content.

TABLE II
Best-Fit Parameters of the Non-Linear Model to the Experiments Figures 11 and 13.

No	K_1 (MPa)	K_2 (MPa)	K_{s1} (MPa)	K_{s2} (MPa)	K_{d1} (10^4 MPa s)	K_{d2} (10^5 MPa s)	K_{d3} (10^3 MPa s)
a	12	12	N/A	N/A	2.1	1.3	N/A
a′	10	8.2	8.0	25	0.82	9.3	1.7
b	12	7.9	6.6	24	0.64	4.4	4.0
c	15	14	7.0	17	0.28	3.1	9.2

Figure 12(a) shows the stress–strain curves for a crosslinked FC2178 sample containing 25 pph SS and 6.0 pph TETA that was first strained to 50%, then released to zero stress and then strained beyond 50%. Notice that the sample has 'memory' of its original behavior (same slope in the stress–strain curve) when it is strained beyond 50%. Figure 12(b) shows the stress–strain curves for two identical films that have been first strained to 40% and then cycled to 15% or 25% strain repeatedly. The data cycled to 15% show no hint of a region of increasing modulus, while there is some increase in modulus when the film is stretched to 25%. A non-linear element is needed that can 'memorize' the deformation history and that has little effect when the strain is small, after an initial high-strain extension.

We propose that the non-linear element resemble the behavior of a string. Carbon black is composed of chains of carbon nano-spheres that can attach one to the next, like filaments. When the polymer is stretched, we believe the carbon black filaments will first rotate to be parallel to the stretching direction. At this point, the 'string' will be taut, and there will be stretching of the polymer attached to the end of the carbon black. If the stress is released, only a small contraction will occur before the stress reaches zero.

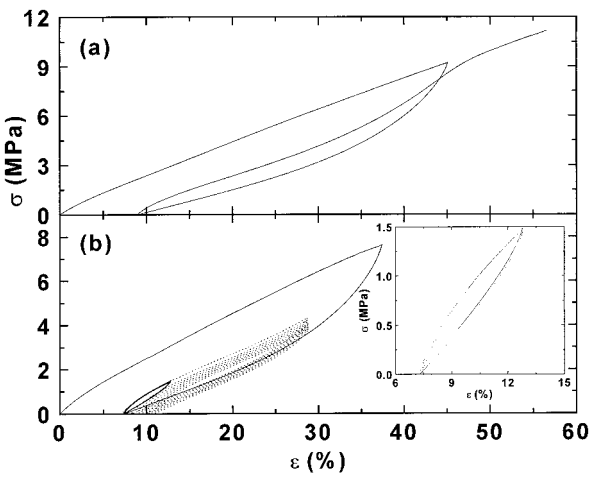

Figure 12 Features that cannot be explained by the linear model: (a) 'memory' effect, and (b) linear and non-linear stress vs. strain of an FC2178 film with 25 pph SS and 6.0 pph TETA.

Figure 3 shows a schematic model of the non-linear element we propose. As the element is stretched (a→b→c→d) the carbon black filaments rotate to be parallel to the stretching direction, thus establishing a new, longer equilibrium length. When the stress is removed, the polymer contracts (d→e→f), but we assume the carbon black strand does not rotate fully back to the original position and the element goes 'slack' at the point *f* in Figure 3. After that, the stress will be zero if the strain is further reduced (f→g→a). Based on the above discussion, a non-linear element was added to the mechanical model (see Fig. 2). The stress within the non-linear element, σ_n, can be described by eq. (1).

Fitting Experiments to the Non-Linear Model

Figure 13 shows stress–strain curves calculated using the non-linear model compared to the data in Figures 11 and 12. The best-fit parameters are listed in Table II (rows a′, b and c respectively). Figure 13(a) shows the fitting to the cyclic stress–strain curve. The non-linear model fits the experimental curve very well. It also

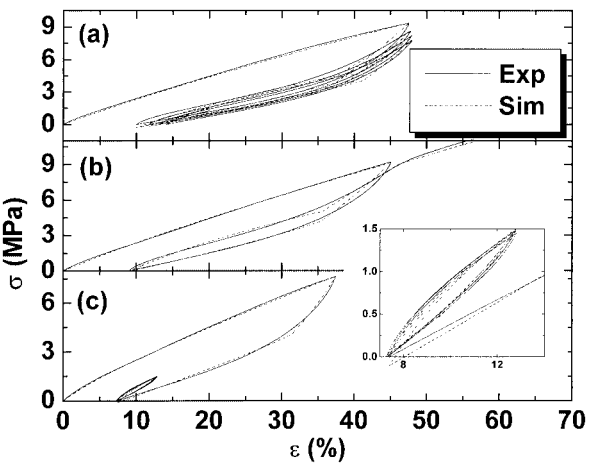

Figure 13 Testing the non-linear model's description of carbon-filled crosslinked FC2178: (a) increase of modulus at large strain during cyclic deformation, (b) 'memory' effect for films cycled once and then strained further, and (c) the linear behavior at small strain after a large initial strain history. The sample used was FC2178 with 25 pph SS and 6.0 pph TETA.

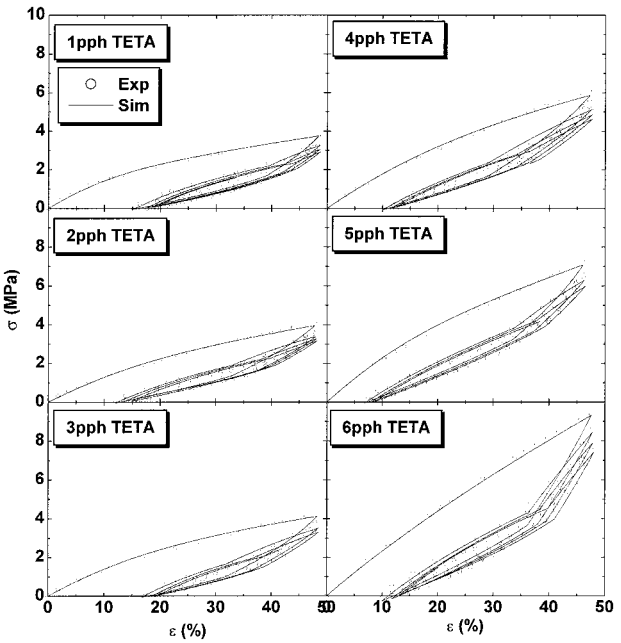

Figure 14 Stress vs. strain curves showing the effect of TETA on the mechanical properties of FC2178 films with 25 pph SS. Best-fit calculations using the non-linear model are also shown.

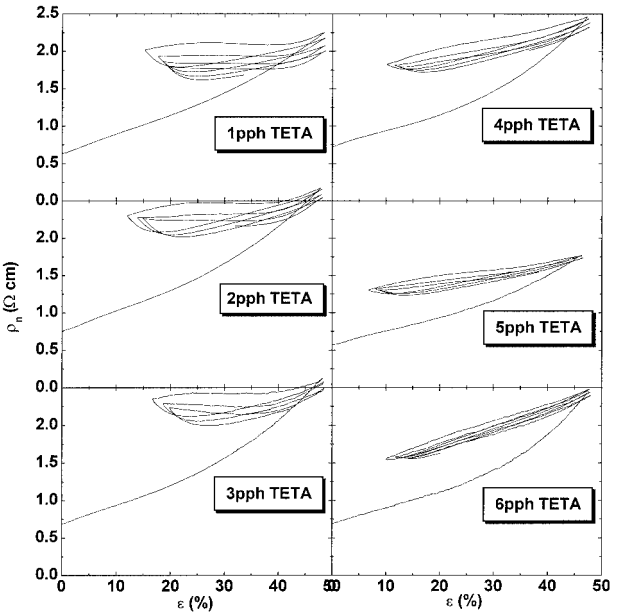

Figure 15 Nominal resistivity vs. strain curves showing the effect of TETA on the electrical properties of FC2178 film with 25 pph SS.

predicts the upturn of the stress at about 40% strain, which is beyond the capability of the linear model. The singular point at about 40% strain occurs at the point where the non-linear element establishes its new equilibrium length. The non-linear model can also predict the 'memory' effect of the polymer film with SS [Fig. 13(b)] and the linear cycling behavior at small strain [Fig. 13(c)]. The parameters listed in Table II provide good fits to the data in Figure 13, but we feel they are not unique in this respect. For example, each of the parameter sets a', b and c in Table II produce stress–strain curves that agree almost exactly during the initial extension. The parameter sets differ slightly in order to fit subsequent behavior.

Effect of TETA on the Properties of FC2178 Films with 25 pph SS

When no TETA was added, the FC2178 film with 25 pph SS easily broke at about 20% strain [see Fig. 7(a)]. The addition of TETA improves the mechanical properties, and all films can be cyclically stretched to 50% strain without breaking. Figure 14 shows stress–strain curves (as open circles) during cyclic deformation for films with different TETA contents. As the TETA content increases, the maximum stress of the films increases from about 4 MPa (1 pph TETA) to about 9 MPa (6 pph TETA). Moreover, the rebound point in the stress–strain curves decreases from 15% to about 10%. Figure 14 also shows the fits to the experiments (as solid lines) using the non-linear model. The non-linear model fits all the experiments quite well. The best-fit parameters are listed in Table III. The parameters K_1, K_{d1} and K_{d3} increase with TETA content.

Figure 15 shows the effect of TETA on the nominal resistivity of the FC2178 films with 25 pph SS. The nominal resistivity of all the samples ranges from 1.5 to 2.5 Ω cm during cyclic deformation. The addition of TETA has no significant impact on the value of nominal resistivity. However, the results clearly demonstrate the effect of TETA on the reversibility of the

TABLE III
The Best-Fit Parameters of the Non-linear Model to Crosslinked FC2178 Films Containing Carbon Black

TETA Content (pph)	K_1 (MPa)	K_2 (MPa)	K_{s1} (MPa)	K_{s2} (MPa)	K_{d1} (10^3 MPa s)	K_{d2} (10^5 MPa s)	K_{d3} (10^3 MPa s)
1.0	4.4	5.8	4.5	7.4	4.0	6.8	0.69
2.0	4.6	4.6	5.0	5.4	4.2	1.5	1.5
3.0	4.8	6.4	4.5	5.2	6.2	4.9	1.5
4.0	5.7	5.2	4.8	6.2	8.4	3.2	3.6
5.0	6.6	4.9	4.3	13	7.8	4.4	4.1
6.0	11	8.4	7.0	15	12	1.6	8.7

polymer. As the TETA content increases, the difference in nominal resistivity between loading and unloading cycles decreases after the first cycle. When 6.0 pph TETA was used, the nominal resistivity changes reversibly during cycling. This may be attributed to crosslinking in the polymer matrix. As the degree of crosslinking increases, the modulus of the polymer matrix increases and the possibility of carbon black reorientation decreases. Hence, the reversibility should increase with TETA content.

CONCLUSIONS

The linear model was used to study the crosslinking of poly(vinylidene fluoride-*co*-hexafluoropropylene). Agreement between the predictions of the linear model and experiment was good for the pure crosslinked polymer. However, the linear model could not describe stress–strain experiments well for the carbon-filled polymer. During cyclic deformation up to 50% strain, the modulus of the polymer/carbon black films increased when the strain was larger than 40%, which cannot be explained by the linear model. Second, the carbon-filled polymer films showed a 'memory' of the previous deformation history that cannot be explained by the linear model. In order to describe the experimental observations, a non-linear model was proposed to describe the mechanical behavior of polymer/carbon black films.

PVDF has poor mechanical properties that may be problematic for applications as an electrode binder when the electrode particles undergo a large volumetric change. FC2178 demonstrated much better mechanical properties and may a potential binder for alloy electrode materials. Addition of a crosslinking agent not only improves the mechanical properties of the polymer and the polymer/carbon black blends, but also improves the reversibility of the electrical properties during cyclic deformation.

The authors acknowledge NSERC, 3M Co. and 3M Canada Co. for funding this work.

References

1. Punkka, E.; Laakso, J.; Stubb, S.; Kuivalainen, P. Phys Rev B 1990, 41, 5914.
2. Zhang, X. W.; Pan, Y.; Zhang, Q.; Yi, X. S. Polym Intern 2001, 50, 229.
3. Taya, M.; Kim, W. J.; Ono, K. Mech Mater 1998, 28, 53.
4. Wen, S.; Wang, S.; Chung, D. D. L. J Mater Sci 2000, 35, 3669.
5. Zhang, S. S.; Jow, T. R. J Power Sources 2002, 109, 422.
6. Fransson, L.; Eriksson, T.; Edström, K.; Gustafsson, T.; Thomas, J. O. J Power Sources 2001, 101, 1.
7. Maleki, H.; Deng, G.; Kerzhner-Haller, I.; Anani, A.; Howard, J. N. J Electrochem Soc 2000, 147, 4470.
8. Lee, B.-L. J Vinyl Techn 1993, 15, 173.
9. Flandin, L.; Prasse, T.; Schueler, R.; Schutle, K.; Bauhofer, W.; Cavaille, J.-Y. Phys Rev B 1999, 59, 14349.
10. Flandin, L.; Hiltner, A.; Baer, E. Polymer 2001, 42, 827.
11. Flandin, L.; Chang, A.; Nazarenko, S.; Hiltner, A.; Baer, E. J Appl Polym Sci 2000, 76, 894.
12. Yamaguchi, M.; Suzuki, K.; Maeda, S. J Appl Polym Sci 2002, 86, 73.
13. Chiou, B.-S.; Schoen, P. E. J Appl Polym Sci 2002, 83, 212.
14. Ganguly, S.; Chakraborty, S.; Banerjee, A. N.; Bhattacharya, P. J Appl Polym Sci 2002, 85, 2025.
15. Baiardo, M.; Frisoni, G.; Scandola, M.; Licciardello, A. J Appl Polym Sci 2002, 83, 38.
16. Severini, F.; Formaro, L.; Pegoraro, M.; Posca, L. Carbon 2002, 40, 735.
17. Beaulieu, L. Y.; Eberman, K. W.; Turner, R. L.; Krause, L. J.; Dahn, J. R. Electrochem Solid-State Lett 2001, 4, A137.
18. Mao, O.; Turner, R. L.; Courtney, I. A.; Fredericksen, B. D.; Buckett, M. I.; Krause, L. J.; Dahn, J. R. Electrochem Solid-State Lett 1999, 2, 3.
19. Idota, Y.; Kubuta, T.; Matsufuji, A.; Maekawa, Y.; Miyasaka, T. Science 1997, 276, 1395.
20. Fang, L.; Chowdari, B. V. R. J Power Sources 2001, 97-98, 181.
21. Shi, L.; Li, H.; Wang, Z.; Huang, X.; Chen, L. J Mater Chem 2001, 11, 1502.
22. Ward, I. M.; Hadley, D. W. An Introduction to the Mechanical Properties of Solid Polymers; Wiley: New York, 1998.